BIOCHEMISTRY
including biophysical chemistry & molecular biology
Article

Biochemistry **2009,** *48,* 6157–6165 6157
DOI: 10.1021/bi9007534

23-Residue C-Terminal α-Helix Governs Kinetic Cooperativity in Monomeric Human Glucokinase

Mioara Larion and Brian G. Miller*

Department of Chemistry and Biochemistry, The Florida State University, Tallahassee, Florida 32306-4390

Received May 1, 2009; Revised Manuscript Received May 26, 2009

ABSTRACT: Human glucokinase is a monomeric enzyme that displays a sigmoidal steady-state kinetic response toward increasing glucose concentrations. The allosteric regulation produced by glucose is postulated to arise from the slow interconversion of multiple enzyme conformations during the course of catalysis. Crystallographic data suggest that structural rearrangements linked to glucokinase cooperativity involve a substrate-induced repositioning of an α-helix (α13) located at the C-terminus of the polypeptide. Here, we show that removal of helix α13 abolishes cooperativity and restores Michaelis−Menten kinetics, while reducing the k_{cat} value of the wild-type enzyme by 160-fold. The impaired catalytic activity of the truncated enzyme is not rescued by the trans addition of a synthetic α13 peptide. Unexpectedly, the $K_{m\ glucose}$ value of a glucokinase variant lacking α13 is equivalent to the $K_{0.5\ glucose}$ value of the full-length enzyme. Glucokinase steady-state kinetics is unaffected by the elongation of α13 via the addition of a C-terminal polyalanine tail. To explore the link between cooperativity and the primary sequence of α13, we randomized seven residues within the helix core. Genetic selection experiments in a glucokinase-deficient bacterium identified a variety of hyperactive α13 variants that display lower $K_{0.5\ glucose}$ values, Hill coefficients near unity, and enhanced equilibrium binding affinities for glucose. The present results demonstrate that α13 plays an essential role in facilitating cooperativity. Our findings also establish a link between the primary amino acid sequence of helix α13 and the functional dynamics of the glucokinase scaffold that are required for allostery.

Glucokinase (hexokinase IV) catalyzes the ATP-dependent phosphorylation of glucose in the first and rate-limiting step of glycolysis in pancreatic β-cells (*1*−*3*). The enzyme exists as a monomer under reacting conditions (*4*), yet displays a sigmoidal steady-state kinetic response toward increasing glucose concentrations (*5*, *6*). This unique mode of substrate-facilitated allosteric regulation is critical to the enzyme's physiological role in maintaining glucose homeostasis in the body. Dysfunction in glucokinase catalysis and/or regulation produces two distinct disease states, maturity onset diabetes of the young (MODY[1]) and persistent hyperinsulinemia of infancy (PHHI) (*7*, *8*). MODY is associated with genetic lesions in *glk* that impair catalytic activity, while PHHI is associated with hyperactive glucokinase variants. The central role of glucokinase in modulating glucose metabolism in the human body has generated intense interest in this enzyme as a potential therapeutic target. Indeed, a number of small-molecule glucokinase activators have been recently described, at least one of which has entered phase I clinical trials as an antidiabetic agent (*9*−*12*).

Several models have been formulated to explain the observance of kinetic cooperativity in monomeric enzymes such as glucokinase. Two prominent theories, the mnemonic mechanism (*13*) and the ligand-induced slow transition (LIST) model (*14*), postulate that cooperativity arises from a substrate-induced conformational change that occurs with a rate constant slower than the turnover number. The existence of multiple enzyme states, combined with their failure to equilibrate during the course of the catalysis, produces sigmoidicity in the reaction rate profile. In support of this postulate, Neet and co-workers have observed a slow ($t_{1/2}$ ∼30 s) change in the intrinsic fluorescence signal of rat liver glucokinase upon exposure to glucose (*15*). A pair of transient state kinetic analyses of glucose binding to human glucokinase also demonstrated that substrate association promotes a conformational change that occurs outside of the catalytic cycle (*16*, *17*). Notably, these studies disagree as to whether the enzyme samples multiple conformational states in the absence of glucose, a mechanistic detail that differentiates the LIST and mnemonic models. A very recent analysis of glucose binding kinetics suggests that human glucokinase may sample a more diverse set of conformational states than initially postulated by the LIST and mnemonic mechanisms (*18*).

The three-dimensional structure of human glucokinase, reported in 2004, provided the first structural insight into the

*To whom correspondence should be addressed. 217 Dittmer Laboratory of Chemistry, Department of Chemistry and Biochemistry, Florida State University, Tallahassee, FL 32306-4390. Tel: (850)-645-6570. Fax: (850)-644-8281. E-mail: miller@chem.fsu.edu.

[1]Abbreviations: MODY, maturity onset diabetes of the young; PHHI, persistent hyperinsulinemic hypoglycemia of infancy; GK, glucokinase; LIST, ligand-induced slow transition; OD, optical density; HEPES, 4-(2-hydroxyethyl)-1-piperazineethanesulfonic acid; DTT, dithiothreitol; IPTG, isopropyl-β-D-thiogalactopyranoside.

Published on Web 05/27/2009

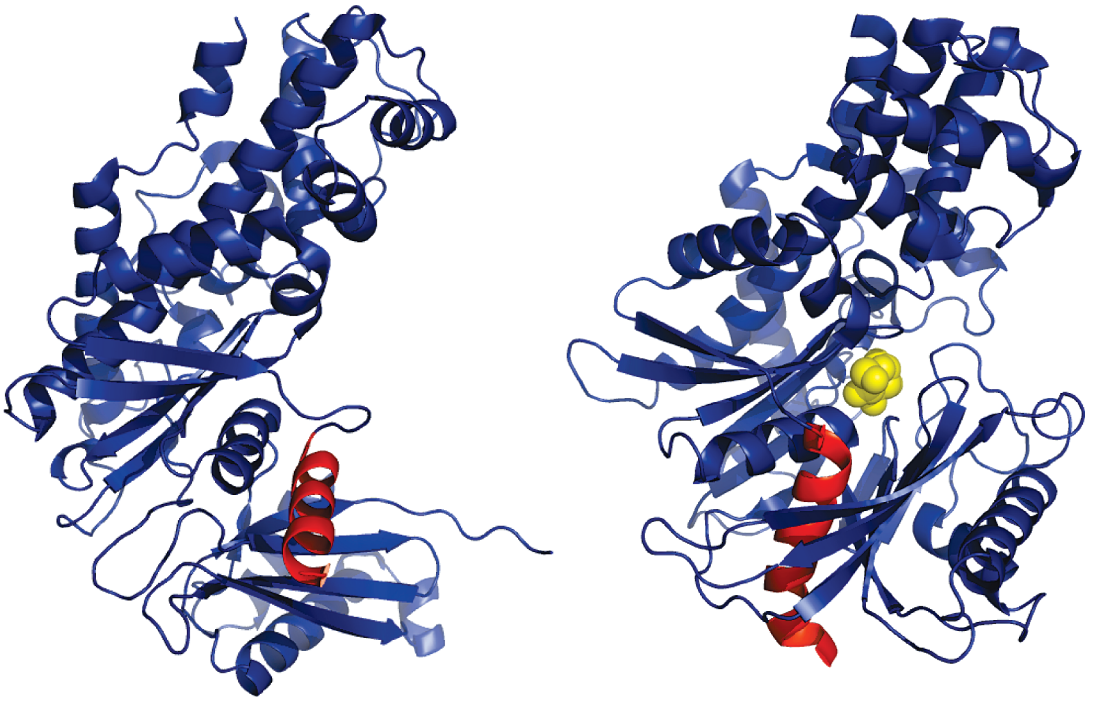

FIGURE 1: Crystal structure of unliganded human glucokinase (left) and glucokinase in complex (right) with glucose (yellow) and an allosteric activator (not shown). Shown in red is helix α13, which moves from a solvent-exposed position in the unliganded structure to a sequestered position upon glucose binding. Images were created with PyMOL (*35*) and PDB entries 1V4T and 1V4S.

conformational changes believed to be linked to the allosteric properties of this enzyme (Figure 1) (*19*). Kamata and co-workers successfully determined the 2.3 Å resolution crystal structure of human hepatic glucokinase in complex with glucose and a synthetic activator. These investigators also determined the structure of unliganded glucokinase at 3.4 Å resolution. The results of these studies revealed a dramatic change in enzyme structure that occurs upon glucose association. When glucose and an activator bind to the human enzyme, the smaller C-terminal domain undergoes a 99° rigid body rotation toward the N-terminal domain, which remains largely stationary. As a result of this conformational change, the enzyme adopts a more compact structure. An important feature of the glucose-induced transition is the position of the helix α13. This secondary structural element, which lies at the C-terminus of the glucokinase polypeptide, moves from a solvent exposed, external orientation in the unliganded structure to an internal, sequestered position in the glucose bound state (Figure 1). The authors speculate that the ability to inhibit the release of this helix from the more compact structure may provide an explanation for the activity of known allosteric effectors. Subsequent molecular dynamics simulations support a model in which the release of helix α13 is the final step in the slow conformational transition from the closed to the super-open conformation (*20*).

Several activating *glk* mutations map to helix α13. These include two naturally occurring substitutions, V455 M and A456 V, identified in patients suffering from PHHI (*21*, *22*), and two variants, S453A and A460R, created *in vitro* (*23*, *24*). In general, these single site variants display decreased cooperativity and lower glucose $K_{0.5}$ values compared to those of the wild-type enzyme, consistent with the hypothesis that helix α13 participates in the conformational transitions that regulate glucokinase activity *in vivo*. Several small molecule allosteric activators also make contact with residues located within α13, demonstrating the importance of this structural feature in therapeutic design. An additional function of α13 has been recently proposed by Flatmark and co-workers, who demonstrated that this secondary structural element constitutes part of a ubiquitin interacting motif (*25*). Thus, helix α13 appears to participate in the post-translational regulation of glucokinase action by mediating proteasomal degradation.

In the present study, we investigate the extent to which helix α13 contributes to the unique kinetic characteristics of human glucokinase. We show that cooperativity can be eliminated by removing α13 or by optimizing its sequence for maximal *in vivo* activity. Combinatorial substitutions in the helix generate polypeptides with equilibrium glucose binding affinities that mirror the high glucose binding affinities of other noncooperative human glucokinase isozymes. Together, these results illuminate the critical role played by α13 in facilitating cooperativity and establish a link between the primary sequence of this structural element and the dynamics of glucokinase conformational rearrangements.

MATERIALS AND METHODS

Site-Directed Mutagenesis. The Asp205Ala variant of human pancreatic glucokinase was constructed using the Quikchange site-directed mutagenesis strategy (Stratagene) using oligonucleotides purchased from Integrated DNA Technologies. Similarly, the Quikchange mutagenesis protocol was used to insert two consecutive amber stop codons after residue 442 in the glucokinase coding sequence. DNA sequencing using primers in both the forward and reverse directions confirmed the successful creation of site-specific variants.

Protein Expression and Purification. Wild-type and variant human pancreatic glucokinases were produced as N-terminal hexa-histidine tagged polypeptides in glucokinase-deficient *E. coli* K-12 strain BM5340(DE3) (*26*). Bacterial cultures were inoculated to an initial $OD_{600\ nm}$ of 0.01 and were grown at 37 °C in Luria−Bertani broth supplemented with ampicillin (150 μg/mL),

kanamycin (40 μg/mL), and chloramphenicol (25 μg/mL). When the $OD_{600\ nm}$ reached 0.85, IPTG (1 mM) was added to induce gene expression, and the temperature was reduced to 20 °C, where growth was continued for 20 h. Cells were harvested by centrifugation at 8,000*g*, and 5 g of wet cell pellet was resuspended in 17 mL of buffer A containing HEPES (50 mM at pH 7.6), KCl (50 mM), imidazole (25 mM), and glycerol (30% w/v). Cells were lysed using a French Press and subjected to centrifugation at 25000*g* at 4 °C for 1 h. The supernatant was immediately loaded onto a 5 mL HisTrap Fast Flow Affinity Column (GE Healthcare) previously equilibrated in buffer A. Following loading, the column was washed with 10 column volumes of buffer A followed by 5 columns of buffer A containing 55 mM imidazole. Glucokinase was eluted with buffer A containing 250 mM imidazole, and the enzyme was dialyzed overnight at 4 °C against 1 L of buffer containing HEPES (50 mM at pH 7.6), KCl (50 mM), glycerol (5% w/v), and dithiothreitol (10 mM). Because of the low expression levels of the truncated variant, an additional purification step was added to eliminate contaminants. Following affinity column purification, the truncated glucokinase variant was injected onto a Superose 6 10/300 gel filtration column (Amersham-Pharmacia) pre-equilibrated in a buffer containing HEPES (50 mM at pH 7.6), KCl (50 mM), and dithiothreitol (10 mM). The gel filtration column was run at a flow rate of 0.02 mL/min, and the fractions that contained the highest $A_{280\ nm}$ readings were pooled and retained for further analysis.

Kinetic Assays. The glucokinase activity of individual enzymes was measured spectrophotometrically at 340 nm by coupling the production of ADP to the oxidation of NADH via the combined action of pyruvate kinase and lactate dehydrogenase. Assays were conducted at 25 °C in reaction mixtures containing HEPES (250 mM at pH 7.6), KCl (50 mM), NADH (0.25 mM), dithiothreitol (5 mM), pyruvate kinase (15 units), lactate dehydrogenase (15 units), ATP (0.1−50 mM), $MgCl_2$ (1.1−51 mM), and glucose (0.05−100 mM). Initial rate data from the first 10% of reaction progress curves were fitted to the Hill equation or the Michaelis−Menten equation, depending upon the substrate under investigation and the extent of cooperativity detected in individual enzymes. Assays involving variable glucose concentrations were conducted at a saturating concentration of ATP, and assays involving variable ATP concentrations were conducted at a saturating concentration of glucose. Assays were initiated by the addition of ATP and were conducted in duplicate for each substrate concentration. The kinetic constants reported herein are the average of data obtained from at least two independent preparations of each enzyme. For the truncated variant, glucokinase activity was additionally measured via the glucose-6-phosphate coupled assay.

Equilibrium Binding Assays. For glucose binding assays, proteins were purified as described above and were dialyzed against HEPES (50 mM at pH 7.6), NaCl (50 mM), DTT (10 mM), and glycerol (5%) prior to data collection. Binding affinities were determined by monitoring the change in fluorescence at 335 nm that occurred in the presence of varying glucose concentrations (0.010−100 mM) following excitation of glucokinase (1 μM full-length; 30 μM truncated) at 280 nm using a 5 nm slit width. Enzyme and glucose were mixed in 0.5 mL, 1 cm path length cuvettes in a buffer containing sodium phosphate (5 mM at pH 7.0), KCl (25 mM), and DTT (10 mM). Reaction mixtures were allowed to equilibrate for several minutes at 25 °C prior to measuring fluorescence emission intensity. Equilibrium binding experiments were performed on a Cary Eclipse Fluorescence Spectrometer housed in the Protein Biochemistry Laboratory in the Institute for Molecular Biophysics. Data were collected in duplicate, averaged, and fitted to the following equation:

$$\Delta F = \frac{\Delta F_{max} \times [glucose]}{K_d + [glucose]}$$

Peptide Rescue Experiments. A 13 amino acid peptide of sequence GSGRGAALVSAVA was synthesized and HPLC purified by Dr. Steven Flemer at the Protein Core Facility at the University of Vermont. The molecular weight of the peptide was determined to be 1116 atomic mass units via electrospray ionization mass spectrometry. The lyophilized peptide was dissolved in a final volume of 1 mL of ddH_2O to give a 10 mM stock. Despite the hydrophobic character of the constituent amino acids, the truncated peptide was readily soluble at this concentration. Addition of peptide in trans was done at the following molar ratios of purified truncated human glucokinase to peptide: 1:1, 1:10, 1:50, 1:100, 1:500, and 1:1000. Assays were performed at 25 and 35 °C in a final volume of 0.5 mL. Reaction mixtures contained HEPES (250 mM at pH 7.6), KCl (50 mM), glucose (100 mM), ATP (30 mM), $MgCl_2$ (31 mM), dithiothreitol (10 mM), NADP+(0.5 mM), glucose 6-phosphate dehydrogenase (5 units), truncated glucokinase (5 μM), and varying concentrations of the peptide. Glucokinase was preincubated with the peptide for 10 min, and then glucose was added. The reaction was incubated for an additional 10 min prior to assay initiation via the addition of ATP. Preincubating the enzyme with glucose, followed by peptide addition did not change the measured reaction rates.

Helix Randomization via Gapped-Duplex Ligation. To facilitate the insertion of a randomized oligonucleotide into the wild-type human glucokinase gene, the Quikchange site-directed mutagenesis procedure was used to install unique *Eag*I and *Sph*I sites within the coding sequence for the α13 helix. A library oligonucleotide, LIB, of sequence 5′-GGCCGGGGCGCG-$(XNK)_7$TGTAAGAAGGCCTGCATG-3′ was designed to encode seven contiguous random amino acids. The base composition of the XNK codon was: X=A(32%)/G(39%)/C(21%)/T(25%), N=A(25%)/G(25%)/C(25%)/T(25%), and K=G(50%)/T(50%) (*27*). Duplex DNA was prepared by annealing the LIB oligonucleotide to two shorter oligonucleotides, HELIX1 and HELIX2, which were complementary to the nonrandom termini of the library oligonucleotide. This procedure generated 5′ and 3′ ends of the duplex DNA that were compatible with the *Eag*I and *Sph*I cleavage sites, respectively. The sequence of HELIX1 was 5′-CGCGCCCC-3′, and HELIX2 was 5′-CAGGCCTTCTTA-CA-3′. Oligonucleotides were ordered from Integrated DNA Technologies and were phosphorylated at the 5′ end. Oligonucleotides LIB (1.5×10^{-11} mol), HELIX1 (2.8×10^{-10} mol), and HELIX2 (2.8×10^{-10} mol) were mixed together in annealing buffer containing Tris-HCl (20 mM at pH 7.0), $MgCl_2$ (2 mM), and NaCl (50 mM). The annealing reaction was heated at 65 °C for 5 min, and the reaction was allowed to cool to room temperature. The resulting duplex DNA contains a gap in the randomized region that was filled in by the endogenous DNA replication machinery of *E. coli* following library transformation.

Template plasmid pBGM101-hGK (10 μg) was digested at 37 °C for 3 h with *Eag*I (15 units) in 1× New England Biolabs reaction buffer 3. Following a 3 h incubation, *Sph*I (5 units) was

added and incubation was continued for 16 h at 37 °C. An additional 5 units of *Sph*I was added, and incubation was continued for an additional 2 h to ensure complete digestion of template DNA. The restriction endonuclease digestion reaction was quenched by heating at 65 °C for 10 min, and the insert was removed by adding the reaction mixture to a Zeba spin column (Pierce) filled with Sephacryl S-500 resin (0.6 mL) (GE Healthcare). Prior to sample addition, the resin was prepared by centrifugation for 1 min at 2500*g*. Purified, restriction endonuclease treated vector DNA was eluted from the column by centrifugation for 2 min at 2500*g*. Duplex DNA and digested vector were ligated by incubation overnight at 14 °C in a reaction mixture containing purified linear plasmid (22 μL), annealed gapped-duplex DNA (10 μL), 1× T4 DNA ligase reaction buffer, and T4 DNA ligase (200 units) (New England Biolabs). Following ligation, sodium acetate (0.3 M pH 4.6) and three volumes of ice-cold ethanol (95% w/v) were added to the reaction. The reaction was incubated for 30 min at −20 °C to promote DNA precipitation, and the sample was centrifuged at 25,000*g* for 10 min. The supernatant was removed, and the pellet was washed with 0.1 mL ice-cold ethanol (70%). The pellet was allowed to air-dry for 10 min at room temperature, resuspended in ddH_2O (15 mL), and desalted by passage across an AutoSeq G50 spin column (GE Healthcare).

Library Analysis. Electrocompetent BM5340(DE3) cells (25 μL) were mixed with the gapped-duplex DNA library (1 μL), and cells were transformed via electroporation. SOC (1 mL) was added, and cells were allowed to recover for 1 h at 37 °C. Serial dilutions were plated on LB agar containing ampicillin (150 μg/mL), kanamycin (40 μg/mL), and chloramphenicol (25 μg/mL), yielding a total of 2.0×10^7 transformants. Following overnight incubation at 37 °C, 12 colonies from the nonselective LB agar plates were picked and inoculated into antibiotic supplemented LB medium (1 mL). Plasmid DNA was prepared from each culture using the Promega Wizard purification kit, and DNA was sequenced at the sequencing facility at Florida State University. Sequence analysis confirmed that more than 95% of the clones harbored a randomized insert.

Genetic Selection. To identify library members with a viable helix sequence, the gapped-duplex library was transformed into electrocompetent BM5340(DE3) cells as described above. Following 1 h of recovery in SOC, cells were transferred to a sterile 2 mL Eppendorf tube and centrifuged for 5 min at 2000*g*. The supernatant was removed, and the pellet was resuspended in M9 minimal medium (1 mL). Centrifugation was repeated at 2000*g*. The washing step was repeated with a second aliquot of M9, and the final pellet was resuspended in 500 μL of M9 minimal medium. Cells were plated in 50 μL aliquots on M9 plates containing glucose (250 μM), IPTG (50 μM), $MgCl_2$ (2 mM), ampicillin (150 μg/mL), kanamycin (40 μg/mL), and chloramphenicol (25 μg/mL). Plates were incubated at 37 °C, and colony growth was monitored closely with the assistance of a hand-held magnifying glass. A small number of colonies were visible within 48 h of plating, at which time colonies were marked. Marked colonies were picked following 72 h of incubation at 37 °C with a 10 μL pipet tip. Colonies were inoculated into antibiotic supplemented LB medium (1 mL), and cultures were grown overnight at 37 °C. Plasmid DNA was purified as described above, and DNA was submitted for sequencing. From our 2×10^7-member library, we picked 40 of the fastest growing colonies, 35 of which returned high quality DNA sequencing results.

RESULTS

Characterization of Truncated Human Glucokinase. To probe the role of the C-terminal α13 helix in glucokinase catalysis and cooperativity, two stop codons were introduced at position 442 of the human pancreatic *glk* gene. The resulting gene product, which lacks the final 23 amino acids of the wild-type polypeptide, was produced in a glucokinase-deficient bacterial host to avoid contamination with endogenous glucokinases. Steady-state kinetic analysis of the purified enzyme indicated that the truncated variant retained a low level of glucokinase activity and displayed standard, hyperbolic Michaelis−Menten kinetics (Figure 2). The k_{cat} value of the truncated variant was 0.18 s^{-1}, a value that is 160-fold lower than the k_{cat} value of the full-length enzyme (Table 1). To verify that the low k_{cat} value measured with this variant was authentic, an additional control experiment was performed. Using site-directed mutagenesis, the putative catalytic active site base, Asp205, was replaced with alanine within the truncated variant. Kinetic assays of the purified D205A variant revealed a further loss of activity (200-fold), demonstrating that the k_{cat} value obtained with the truncated enzyme provides a true measure of this enzyme's catalytic ability. The glucose K_m value displayed by the truncated variant was 5 mM, which closely matches the $K_{0.5}$ value (8 mM) of the wild-type enzyme. In contrast, the ATP K_m value of the truncated variant was elevated by 10-fold compared to that of the wild-type enzyme.

We assessed the ability of truncated glucokinase activity to be rescued via the trans addition of a 13 amino acid peptide with a sequence that matches that of the endogenous α13 helix. Incubation of the truncated variant with increasing concentrations of the

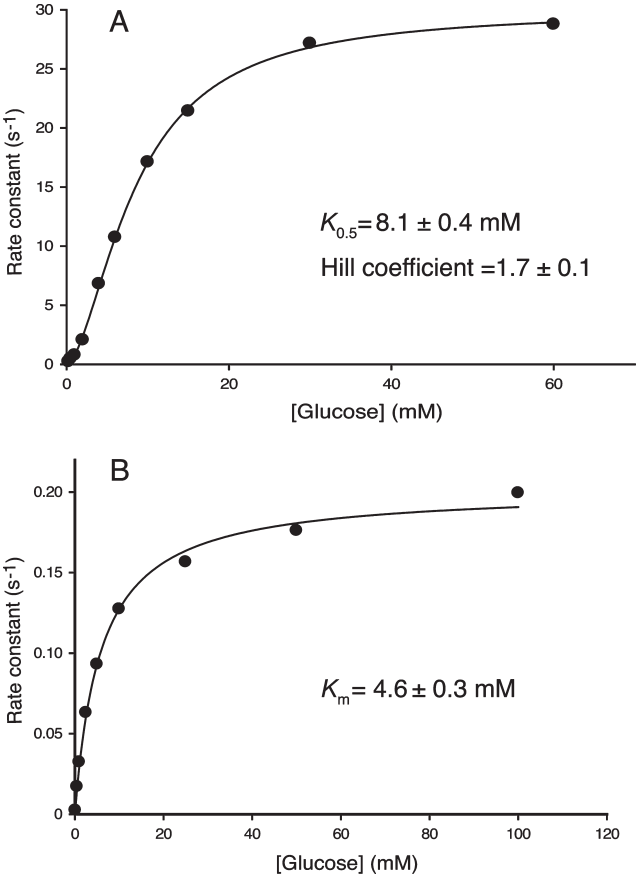

FIGURE 2: Comparison of the steady-state kinetics of cooperative wild-type human glucokinase (A) and a noncooperative truncated variant lacking helix α13 (B).

Table 1: Kinetic and Thermodynamic Parameters of Wild-Type GK, Truncated GK, and the Truncated D205A Variant

parameter	wild-type GK	truncated GK	D205A truncated GK
k_{cat} (s^{-1})	29 ± 1	0.18 ± 0.01	$< (9.1 \pm 0.7) \times 10^{-4}$
$K_{0.5\ glucose}$ (M)	$(8.1 \pm 0.4) \times 10^{-3}$	$(5.2 \pm 0.5) \times 10^{-3}$	n.d.[a]
$k_{cat}/K_{0.5\ glucose}$ ($M^{-1}\ s^{-1}$)	$(3.6 \pm 0.1) \times 10^{3}$	$(3.5 \pm 0.1) \times 10^{1}$	n.d.
Hill coefficient	1.7 ± 0.1	0.9 ± 0.05	n.d.
$K_{D\ glucose}$ (M)	$(2.9 \pm 0.2) \times 10^{-3}$	$(7.6 \pm 2.4) \times 10^{-4}$	n.d.

[a] n.d., not determined.

Table 2: Effects on k_{cat} upon Peptide Addition to Truncated GK at 25°C and 35°C

molar ratio wt-hGK/peptide	temperature (°C)	fold increase in k_{cat}
1:0	25	1
1:1	25	1.1
1:10	25	1.2
1:100	25	1.2
1:500	25	1.5
1:1000	25	1.6
1:500	35	1.4

purified synthetic peptide at ratios ranging from 1:1 to 1:1000 did not reveal substantial levels of reactivation. The turnover number for glucose phosphorylation measured at 25 °C showed a modest 1.6-fold increase in the presence of high concentrations of peptide (5 mM). Increasing the temperature of the incubation to 35 °C did not significantly increase the k_{cat} value of the truncated enzyme (Table 2).

To investigate the effect of α13 removal upon the equilibrium binding affinity for substrate glucose, the fluorescence emission spectrum of truncated glucokinase was obtained in the absence and presence of 100 mM glucose. High concentrations of enzyme (30 μM) were required in these experiments, as the emission spectrum of the truncated variant displayed a very small increase in intensity following glucose addition. A shift toward shorter wavelengths was observed in the emission spectrum of the truncated variant upon exposure to glucose (Figure 3). These observations contrast with the effect of glucose binding to the wild-type enzyme, which causes a significant increase in the fluorescence intensity and does not alter the λ_{max} of the emission spectrum. The truncated variant displays an apparent glucose dissociation constant of 760 μM, a value that is 3.8-fold lower than the glucose equilibrium binding affinity measured with the full-length enzyme (Table 1). Thus, removal of α13 causes a small decrease in both the glucose $K_{0.5}$ and K_D values when compared with those of the wild-type enzyme.

Elongation of the α13 Helix. A comparison of the crystal structure of human glucokinase in the presence and absence of bound glucose and an allosteric activator suggested that lengthening helix α13 might impede the interconversion of these two conformational states (Figure 4) (*19*). To investigate that possibility, we added 5 and 10 alanine residues to the C-terminus of the wild-type glucokinase polypeptide. Steady-state kinetic assays of the purified elongated variants revealed that neither addition significantly altered the kinetic constants of the wild-type enzyme (Table 3). The cooperativity of the enzyme was also unaffected by α13 elongation.

Randomization of the α13 Helix. To explore the sequence requirements of α13, we constructed a genetic library in which all 20 amino acids were allowed to occupy 7 consecutive residues (450−456) within the helix core. Transformation of this library into the glucokinase-deficient BM5340(DE3) strain yielded 2×10^7 members, representing 1.5% of the theoretical 1.28×10^9 member library. Sequencing of clones isolated from the nonselective medium confirmed the randomness of the library. To identify active α13 variants, transformed BM5340(DE3) cells were challenged for growth on glucose minimal medium. Forty of the fastest growing colonies were picked, and the plasmid DNA was sequenced to determine the identity of α13 residues. High quality sequencing data was returned from 35 selected clones. In general, the substitutions observed in positions 450−456 were dominated by amino acids that have a statistically significant preference for adopting an α-helical structure. From a total of 245 different positions observed in the 35 selected enzymes, 69% (168/245) were occupied by 1 of 7 helix stabilizing amino acids (A, E, K, L, M, Q, and R) (*28*). An additional 18% (43/245) of positions were filled with residues that lack a strong conformational preference, while 14% were occupied by residues that could be considered helix destabilizing (G, C, N, P, S, T, and Y). Charged amino acids were observed in 4.4% (11/245) of selected helix residues, whereas 76% of the 245 positional variants were occupied by hydrophobic amino acids.

The primary sequence of clones that provided high quality sequencing data is summarized in Table 4. Residue 450, an alanine in the wild-type enzyme, was highly conserved in the selected α13 variants. Alanine (66% occupancy) and glycine (34% occupancy) were the only permissible amino acids at this position. Residue 451 was also highly conserved. Eighty percent of the selected α13 helix variants possessed the native leucine at this position. The occupancy of residue 452 was dominated by three hydrophobic amino acids: leucine, isoleucine, and the native valine. Leucine was the most common substitution observed at residue 452, with 51% of selected sequences possessing this amino acid. Residue 453, occupied by serine in the wild-type enzyme, was nearly always substituted in the selected variants, most often by alanine (74% occupancy) or valine (23%). Residues 454−456 were more highly variable than residues 450−453. At residue 454, methionine was observed in 37% of selectants, while the native alanine was retained in 23% of selected clones. Twelve different amino acids were observed at residue 455, with arginine occurring most frequently (20% occupancy). Notably, the wild-type valine was never observed in our selected sequences, and the known activating substitution V455 M was only observed twice. Nine different amino acids were found to occupy residue 456, the final position randomized in our library. A naturally occurring A456 V variant has been observed in patients suffering from PHHI. This substitution was observed in 17% of our selectants; however, other hydrophobic amino acids including leucine, isoleucine, and methionine account for an additional 60% of residue 456 occupants.

To evaluate the kinetic and thermodynamic properties of α13 variants identified by our genetic selection experiments, we chose three enzymes for further characterization that best represented

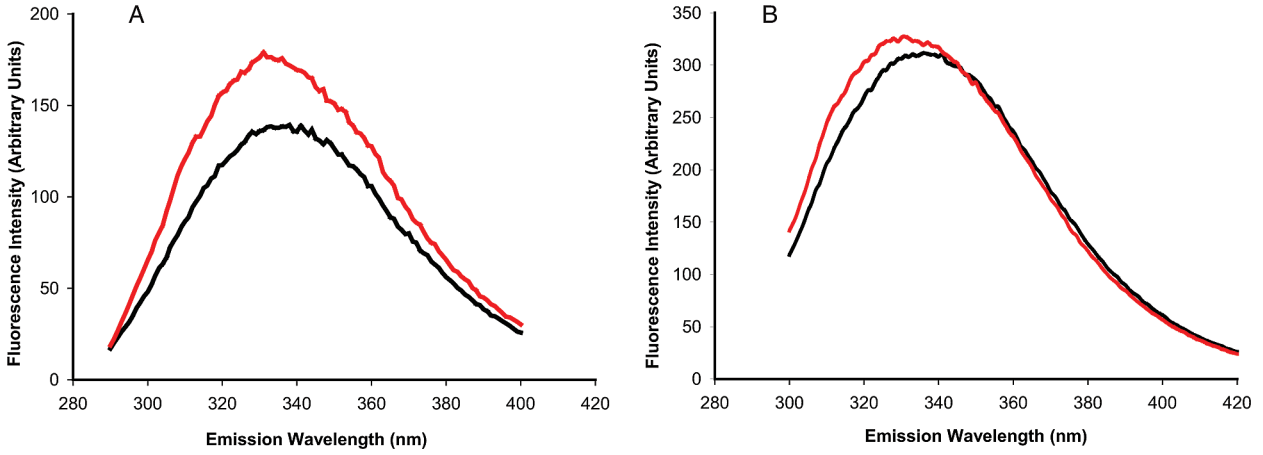

FIGURE 3: (A) Fluorescence emission spectrum of wild-type human glucokinase (1 μM) in the absence (black) and presence (red) of 0.1 M glucose. (B) Fluorescence emission spectrum of truncated human glucokinase (30 μM) in the absence (black) and presence (red) of 0.1 M glucose.

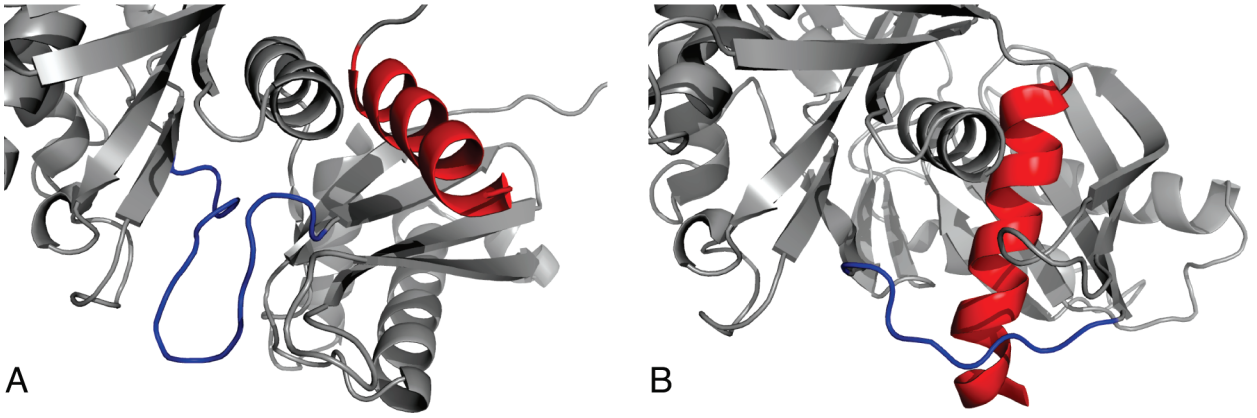

FIGURE 4: Position of helix α13 (red) and the connecting loop (blue) in the structure of (A) unliganded human glucokinase and (B) glucokinase crystallized in the presence of glucose and an allosteric activator, suggesting that elongation of α13 might impede the conformational transition between these states. Images were created with PyMOL (*35*) and PDB entries 1V4T and 1V4S.

Table 3: Catalytic Effects of C-Terminal Polyalanine Addition

parameter	wild-type GK	GK + 5 alanine	GK + 10 alanine
k_{cat} (s^{-1})	29 ± 0.1	37 ± 5	38 ± 8
$K_{0.5\ glucose}$ (M)	(8.1 ± 0.4) × 10^{-3}	(10 ± 1) × 10^{-3}	(10.5 ± 0.5) × 10^{-3}
$k_{cat}/K_{0.5\ glucose}$ ($M^{-1}\ s^{-1}$)	(3.6 ± 0.1) × 10^{3}	(3.7 ± 0.1) × 10^{3}	(3.6 ± 0.7) × 10^{3}
Hill coefficient	1.7 ± 0.1	1.6 ± 0.2	1.7 ± 0.1
$K_{m\ ATP}$ (M)	(5.0 ± 0.1) × 10^{-4}	(5.2 ± 0.5) × 10^{-4}	(4.2 ± 0.1) × 10^{-4}
$k_{cat}/K_{m\ ATP}$ ($M^{-1}s^{-1}$)	(5.6 ± 0.1) × 10^{4}	(6.9 ± 1.2) × 10^{4}	(8.9 ± 0.9) × 10^{4}

the most common positional substitutions observed in our selected library members. The primary sequence of the randomized region of the chosen variants was ALIAAAV, ALLAMAV, and ALVASRL. Steady-state assays of these three variants showed that each displayed a 6−10-fold decrease in the wild-type $K_{0.5\ glucose}$ value, while none possessed a substantially altered k_{cat} value (Table 5). The degree of cooperativity, as measured by the Hill coefficient, is substantially decreased in each of the α13 variants, and the ATP K_m value is decreased by approximately 3-fold for each variant. In general, these kinetic characteristics match those observed in other activated human glucokinase variants. Optimizing the sequence of helix α13 also had a striking effect upon the equilibrium binding affinity for glucose. Compared to the wild-type enzyme, the ALIAAAV and ALLAMAV variants showed a 60-fold increase in glucose binding affinity, while the ALVASRL variant displayed a more modest 4-fold increase in affinity.

DISCUSSION

The purpose of the present study was to investigate the contribution of the C-terminal α13 helix of human glucokinase to the kinetic characteristics of this enzyme. Here, we show that loss of helix α13 produces a large decrease in the k_{cat} value of the wild-type enzyme, demonstrating the essentiality of this structural element to catalytic turnover. We also observe a complete loss of kinetic cooperativity upon removal of helix α13. The mnemonic and LIST models postulate that monomeric cooperativity in glucokinase results from a slow alteration in enzyme structure (*13*, *14*). The reduced k_{cat} value of the truncated enzyme suggests that the rate of the chemical step is sufficiently reduced

Table 4: Identity and Frequency of Amino Acids Observed at Positions 450−456 Following Genetic Selection for *E. coli* Growth of a Randomized α13 Helix Library[a]

alanine 450	leucine 451	valine 452	serine 453	alanine 454	valine 455	alanine 456
66% Ala*	80% Leu*	51% Leu*	74% Ala*	37% Met*	20% Arg*	26% Leu*
34% Gly	8.5% Met*	23% Val	20% Val	23% Ala*	20% Gln*	20% Met*
	8.5% Ile	17% Ile	3% Cys	11% Arg*	17% Gly	17% Val
	3% Phe	6% Ala*	3% Ser	11% Ser	11% Ala*	14% Ile
		3% Cys		6% His	6% Asn	6% Ala*
				6% Leu*	6% Cys	6% Thr
				3% Gln*	6% Met*	3% Gln*
				3% Tyr	3% Asp	3% Glu*
					3% Ile	3% His
					3% Ser	
					3% Trp	
					3% Tyr	

[a] Previously described activating substitutions are underlined. Substitutions that are expected to stabilize the α13 helix based upon amino acid conformational preferences are denoted with an asterisk.

Table 5: Kinetic and Thermodynamic Characterization of Selected α13 Variants

parameter	wild-type (ALVSAVA)	variant #1 (ALIAAAV)	variant #2 (ALLAMAV)	variant #3 (ALVASRL)
k_{cat} (s^{-1})	29 ± 0.1	17 ± 2.4	18 ± 0.2	29 ± 0.2
$K_{0.5\ glucose}$ (M)	$(8.1 \pm 0.4) \times 10^{-3}$	$(1.0 \pm 0.1) \times 10^{-3}$	$(0.8 \pm 0.1) \times 10^{-3}$	$(1.4 \pm 0.1) \times 10^{-3}$
$k_{cat}/K_{0.5\ glucose}$ ($M^{-1}\ s^{-1}$)	$(3.6 \pm 0.1) \times 10^{3}$	$(1.7 \pm 0.1) \times 10^{4}$	$(2.2 \pm 0.3) \times 10^{4}$	$(2.2 \pm 0.3) \times 10^{4}$
fold increase $k_{cat}/K_{0.5\ glucose}$	1	5	6	6
Hill coefficient	1.7 ± 0.1	1.2 ± 0.2	1.1 ± 0.2	1.2 ± 0.1
$K_{m\ ATP}$ (M)	$(5.0 \pm 0.1) \times 10^{-4}$	$(1.6 \pm 0.1) \times 10^{-4}$	$(1.6 \pm 0.1) \times 10^{-4}$	$(2.6 \pm 0.1) \times 10^{-4}$
$k_{cat}/K_{m\ ATP}$ ($M^{-1}s^{-1}$)	$(5.6 \pm 0.1) \times 10^{4}$	$(1.3 \pm 0.1) \times 10^{5}$	$(1.1 \pm 0.1) \times 10^{5}$	$(1.2 \pm 0.2) \times 10^{5}$
$K_{D\ glucose}$ (M)	$(2.9 \pm 0.2) \times 10^{-3}$	$(4.9 \pm 1.9) \times 10^{-5}$	$(5.3 \pm 0.9) \times 10^{-5}$	$(6.7 \pm 0.2) \times 10^{-4}$
fold decrease $K_{D\ glucose}$	1	60	55	4

such that the conformational changes associated with glucose binding and/or product release have time to reach equilibrium. This appears to be the most probable explanation for the lack of cooperativity displayed by the truncated glucokinase variant. Alternatively, elimination of helix α13 may prevent the formation of alternate enzyme conformations. Qualitatively, this postulate appears to be supported by the failure of glucose to induce a significant change in intrinsic protein fluorescence in the truncated variant. However, the latter observation can also be explained, in part, by the fact that α13 is located in close proximity to W99, a residue that contributes substantially to the overall fluorescence intensity of wild-type glucokinase (*29*). Thus, α13 removal likely causes a local perturbation in the solvent accessibility of W99, which may explain why the fluorescence emission spectrum of the truncated variant changes little upon glucose binding.

Cooperativity is also reduced when the primary amino acid sequence of α13 is optimized for maximal *in vivo* activity following genetic selection. On the basis of the results tabulated in Table 4, maximal activity appears to correlate with a core α13 sequence that is dominated by hydrophobic amino acids that possess a conformational preference for adopting a helical structure. To understand how cooperativity is lost in the sequence-optimized α13 variants, it is useful to examine the details of both the mnemonic and LIST mechanisms. In the mnemonic mechanism, the conformational change that produces steady-state cooperativity occurs at the conclusion of the catalytic event, when the enzyme forgets its active conformation and slowly relaxes to an alternate conformation. In this model, cooperativity can be reduced by a perturbation of the rate constant that governs the relaxation event. For example, the Hill coefficient will approach unity if the relaxation rate is enhanced such that the conformational states of the enzyme equilibrate prior to the initiation of another catalytic cycle. Alternatively, the Hill coefficient will approach unity if the relaxation rate is reduced to such an extent that the alternate enzyme conformation is rarely sampled. A similar situation facilitates a loss of cooperativity in the LIST model, in which the enzyme is postulated to exist in multiple catalytically competent conformations prior to glucose binding. An acceleration of the rate of conformational interconversions or a perturbation in the conformational equilibrium constant in favor of a single state is expected to produce a Hill coefficient near unity. The hyperactive α13 variants characterized in this study display a substantial increase in glucose binding affinity, similar to those observed in other hexokinases that do not appear to sample multiple unliganded conformations. On the basis of this observation, we postulate that an optimal α13 sequence may eliminate cooperativity by altering the conformational equilibrium of human glucokinase in favor of fewer states.

As shown in Figure 4, α13 moves from a solvent exposed position in the absence of substrate to a sequestered position when both glucose and an allosteric activator are bound to the enzyme. To obtain the bound structure, α13 appears to insert itself behind the connecting loop, which comprises residues 63−72. One full turn of the α13 helix extends beyond the border established by the position of the connecting loop. On the basis of this observation, we postulated that extending α13 would either (a) trap the enzyme in the bound state by preventing helix release or (b) prevent the formation of this state by impeding the insertion of the helix behind the connecting loop. Either of these situations is expected to alter the kinetic characteristics of the

enzyme; however, the enzyme was impervious to the addition of alanine residues to the C-terminus. This finding is consistent with previous reports indicating that a fully active and cooperative enzyme can be obtained when human glucokinase is produced as a C-terminal fusion with the 25-kDa glutathione *S*-transferase (*30*). These observations are difficult to reconcile with the picture of α13-associated conformational changes that emerge from a comparison of the unliganded and glucose-bound structures. It is worth noting that the liganded structure depicted in Figure 4B includes an allosteric activator molecule not shown, which forms contacts with residues in both the helix and the connecting loop. It is likely that the presence of the activator influences the relative positions of the helix and/or the loop. Given these considerations, we speculate that the relative orientation of the connecting loop and α13 is different from those depicted in the currently available crystal structures when the catalytically relevant, glucose bound state is achieved. A full understanding of the interplay of α13 with the connecting loop at various stages of the catalytic cycle awaits the determination of the structure of glucose-bound enzyme in the absence of an activator molecule.

The ability of helix α13 to control the allosteric properties of human glucokinase appears to be a common feature of this polypeptide scaffold. Human hexokinase I, an isozyme of glucokinase, is a 100 kDa enzyme composed of two fused 50 kDa domains connected by a helix analogous to α13 (Figure 5) (*1*). The N-terminal domain of hexokinase I is inactive but contains a binding site for the product glucose 6-phosphate, an allosteric effector that alters activity in the C-terminal catalytic domain. When glucose-6-phosphate binds to the allosteric site, it forms a hydrogen bond with the side chain of Ser449, which is located in the first turn of the connecting helix (*31*). This interaction initiates a 6° rotation of the N-terminal domain with respect to the catalytic C-terminal domain, a conformational change that is propagated to the active site via the alteration of several interdomain contacts. Elongation of the connecting helix or disruption of the helical structure via destabilizing

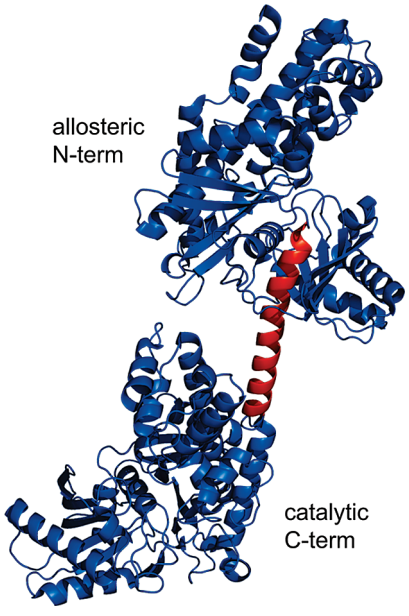

FIGURE 5: Structure of human hexokinase I, an isozyme of glucokinase, depicting the location of the connecting helix (red) that facilitates communication between the allosteric N-terminal domain and the catalytic C-terminal domain.

substitutions has been shown to impede allosteric communication and disrupt the ability of inorganic phosphate to relieve feedback inhibition caused by glucose-6-phosphate binding to the N-terminal allosteric domain (*32*−*34*). Although this regulatory mechanism is distinct from the α13-associated slow conformational changes that produce cooperativity in glucokinase, the role of the helix in facilitating the allosteric properties of each enzyme is functionally conserved.

The findings presented herein demonstrate the importance of helix α13 to the allosteric properties of human glucokinase. Because cooperativity is so intimately linked to both the presence and primary amino acid sequence of α13, this structural element appears to be an ideal site for the attachment of probes to report on the molecular details of enzyme functional dynamics. The placement of spectroscopic labels or NMR sensitive nuclei within α13 promises to facilitate the direct measurement of the rates and magnitudes of structural alterations during various stages of the catalytic cycle. Such information is essential to assembling a complete kinetic, structural, and mechanistic description of cooperativity in this monomeric enzyme.

REFERENCES

(1) Wilson, J. E. (1995) Hexokinases. *Rev. Physiol. Biochem. Pharmacol. 126*, 65–198.
(2) Lowry, O. H., and Possoneau, J. V. (1964) The relationships between substrates and enzymes of glycolysis in brain. *J. Biol. Chem. 239*, 31–42.
(3) Ferre, T., Riu, E., Bosch, F., and Valera, A. (1996) Evidence from transgenic mice that glucokinase is rate limiting for glucose utilization in the liver. *FASEB J. 10*, 1213–1218.
(4) Cardenas, M., Rabajille, E., and Niemeyer, H. (1978) Maintenance of the monomeric structure of glucokinase under reacting conditions. *Arch. Biochem. Biophys. 190*, 142–148.
(5) Parry, M. J., and Walker, D. G. (1967) Further properties and possible mechanism of action of adenosine 5′-triphosphate-D-glucose 6-phosphotransferase from rat liver. *Biochem. J. 105*, 473–482.
(6) Storer, A. C., and Cornish-Bowden, A. (1976) Kinetics of rat liver glucokinase: co-operative interactions with glucose at physiologically significant concentrations. *Biochem. J. 159*, 7–14.
(7) Vionnet, N., Stoffel, M., Takeda, J., Yasuda, K., Bell, G. I., Zouali, H., Lesage, S., Velho, G., Iris, F., Passa, P., Froguel, P., and Cohen, D. (1992) Nonsense mutation in the glucokinase gene causes early-onset non-insulin-dependent diabetes mellitus. *Nature 356*, 721–722.
(8) Golyn, A. (2003) Glucokinase (GCK) mutations in hyper- and hypoglycemia: maturity-onset diabetes of the young, permanent neonatal diabetes, and hyperinsulinemia of infancy. *Hum. Mutat. 22*, 353–362.
(9) Grimsby, J., Sarabu, R., Corbett, W. L., Haynes, N.-E., Bizzarro, F. T., Coffey, J. W., Guertin, K. R., Hilliard, D. W., Kester, R. F., Mahaney, P. E., Marcus, L., Qi, L., Spence, C. L., Tengi, J., Magnuson, M. A., Chu, C. A., Dvorozniak, M. T., Matschinsky, F. M., and Grippo, J. F. (2003) Allosteric activators of glucokinase: potential role in diabetes therapy. *Science 301*, 370–373.
(10) Johnson, T. O., and Humphries, P. S. (2006) Glucokinase activators for the treatment of type 2 diabetes. *Annu. Rep. Med. Chem. 41*, 141–154.
(11) Coope, G. J., Atkinson, A. M., Allott, C., McKerrecher, D., Johnstone, C., Pike, K. G., Holme, P. C., Vertigan, H., Gill, D., Coghlan, M. P., and Leighton, B. (2006) Predictive blood glucose lowering efficacy by glucokinase activators in high fat fed female Zucker rats. *Br. J. Pharmacol. 149*, 328–335.
(12) Guertin, K. R., and Grimsby, J. (2006) Small molecule glucokinase activators as glucose lowering agents: a new paradigm for diabetes therapy. *Curr. Med. Chem. 13*, 1839–1843.
(13) Richard, J., Meunier, J.-C., and Buc, J. (1974) Regulatory behavior of monomeric enzymes 1. The mnemonical enzyme concept. *Eur. J. Biochem. 49*, 195–208.
(14) Ainslie, G. R., Shill, J. P., and Neet, K. E. (1972) Transients and cooperativity: a slow transition model for relating transients and cooperative kinetics of enzymes. *J. Biol. Chem. 247*, 7088–7096.

(15) Lin, S.-X., and Neet, K. E. (1990) Demonstration of a slow conformational change in liver glucokinase by fluorescence spectroscopy. *J. Biol. Chem. 265*, 9670–9675.
(16) Heredia, V., Thomson, J., Nettleton, D., and Sun, S. (2006) Glucose-induced conformational changes in glucokinase mediate allosteric regulation: transient kinetic analysis. *Biochemistry 45*, 7553–7562.
(17) Kim, Y. B., Kalinowski, S. S., and Marcinkeviciene, J. (2007) A pre-steady state analysis of ligand binding to human glucokinase: evidence for a preexisting equilibrium. *Biochemistry 46*, 1423–1431.
(18) Antoine, M., Boutin, J. A., Ferry, G. (2009) Binding kinetics of glucose and allosteric activators to human glucokinase reveal multiple conformational states, Biochemistry [Online early access], DOI: 10.1021/bi900374c, published online Apr 28, 2009.
(19) Kamata, K., Mitsuya, M., Nishimura, T., Eiki, J., and Nagata, Y. (2004) Structural basis for allosteric regulation of the monomeric allosteric enzyme human glucokinase. *Structure 12*, 429–438.
(20) Zhang, J., Li, C., Chen, K., Zhu, W., Shen, X., and Jiang, H. (2006) Conformational transition pathway in the allosteric process of human glucokinase. *Proc. Natl. Acad. Sci. U.S.A. 103*, 13368–13373.
(21) Glaser, B., Kesavan, P., Heyman, M., Davis, E., Cuesta, A., Buchs, A., Stanley, C. A., Thornton, P. S., Permutt, M. A., Matschinsky, F. M., and Herold, K. C. (1998) Familial hyperinsulinism caused by an activating glucokinase mutation. *N. Engl. J. Med. 338*, 226–230.
(22) Christesen, H. B. T., Jacobsen, B. B., Odili, S., Buettger, C., Cuesta-Munoz, A., Hansen, T., Brusgaard, K., Massa, O., Magnuson, M. A., Shiota, C., Matschinsky, F. M., and Berbetti, F. (2002) The second activating glucokinase mutation (A456V). *Diabetes 51*, 1240–1246.
(23) Pedelini, L., Garcia-Gimeno, A., Marina, A., Gomez-Zumaquero, J., Rodriguez-Bada, P., Lopez-Enriquez, S., Soriguer, F., Cuesta-Munoz, A., and Sanz, P. (2005) Structure-function analysis of the α5 and the α13 helices of human glucokinase: description of two novel activating mutations. *Protein Sci. 12*, 2080–2086.
(24) Pal, P., and Miller, B. G. (2009) Activating mutations in the human glucokinase gene revealed by genetic selection. *Biochemistry 48*, 814–816.
(25) Bjorkhaug, L., Molnes, J., Sovik, O., Njostad, P. R., and Flatmark, T. (2007) Allosteric activation of human glucokinase by free polyubiquitin chains and its ubiquitin-dependent cotranslational proteasomal degradation. *J. Biol. Chem. 282*, 22757–22764.
(26) Miller, B. G., and Raines, R. T. (2005) Reconstitution of a defunct glycolytic pathway via recruitment of ambiguous sugar kinases. *Biochemistry 44*, 10776–10783.
(27) Smith, B. D., and Raines, R. T. (2008) Genetic selection for peptide inhibitors of angiogenin. *Prot. Eng., Des. Sel. 21*, 289–294.
(28) Williams, R. W., Chang, A., Juretic, D., and Loughran, S. (1987) Secondary structure predictions and medium range interactions. *Biochim. Biophys. Acta 916*, 200–204.
(29) Zelent, B., Odili, S., Buettger, C., Shiota, C., Grimsby, J., Taub, R., Magnuson, M. A., Vanderkooi, J. M., and Matschinsky, F. M. (2008) Sugar binding to recombinant wild-type and mutant glucokinase monitored by kinetic measurement and tryptophan fluorescence. *Biochem. J. 413*, 269–280.
(30) Liang, Y., Kesavan, P., Wang, L.-Q., Niswender, K., Tanizawa, Y., Permutt, M. A., Magnuson, M. A., and Matschinsky, F. M. (1995) Variable effects of maturity-onset-diabetes-of-youth (MODY)-associated glucokinase mutations on substrate interactions and stability of the enzyme. *Biochem. J. 309*, 167–173.
(31) Aleshin, A. E., Kirby, C., Liu, X., Bourenkov, G. P., Bartunik, H. D., Fromm, H. J., and Honzatko, R. B. (2000) Crystal structures of mutant monomeric hexokinase I reveal multiple ADP binding sites and conformational changes relevant to allosteric regulation. *J. Mol. Biol. 296*, 1001–1015.
(32) Hashimoto, M., and Wilson, J. E. (2002) Kinetic and regulatory properties of HK I+, a modified form of the type I isozyme of mammalian hexokinase in which interactions between the N- and C-terminal halves have been disrupted. *Arch, Biochem. Biophys. 399*, 109–115.
(33) Sui, D., and Wilson, J. E. (2002) Functional interactions between noncovalently associated N- and C-terminal halves of mammalian Type I hexokinase. *Arch. Biochem. Biophys. 401*, 21–28.
(34) Tsai, H. J. (2007) Function of interdomain α-helix in human brain hexokinase: covalent linkage and catalytic regulation between N- and C-terminal halves. *J. Biomed. Sci. 14*, 195–202.
(35) Delano, W. L. (2002) The PyMOL Molecular Graphics System, Delano Scientific, Palo Alto, CA.